Characterization of the π^0 decay via two-photon detection in the proposed sPHENIX forward instrumentation

Brookhaven National Laboratory, USA

Ezra Douglas Lesser

A thesis presented for the partial completion of the requirements for the degree of Bachelor of Science in Physics with Honors

Department of Physics
College of Literature, Science, and the Arts
University of Michigan
Ann Arbor, Michigan, USA
March 11, 2018

Characterization of the π^0 decay via two-photon detection in the proposed sPHENIX forward instrumentation

Ezra D. Lesser
Department of Physics, University of Michigan

Abstract

The sPHENIX experiment at the Relativistic Heavy Ion Collider (RHIC) at Brookhaven National Laboratory (BNL) in New York, USA will have new forward instrumentation, partially refurbished and repurposed from the PHENIX experiment, with one of many physics goals being the measurement of direct photons from partonic hard scattering. These electroweak emissions, which are rarer than dijets from strong processes, are excellent probes for experimentally testing the theory of quantum chromodynamics (QCD), studying the quark-gluon plasma (QGP), measuring single and double spin asymmetries, and quantifying factorization breaking of nonperturbative functions. However, the direct photon signal will be overwhelmingly dominated by background from jets, and correctly identifying this large background from initial-state hadrons is critical to extracting meaningful physics via the direct photon signal. The largest component of this background, the $\pi^0 \to \gamma\gamma$ decay, will be difficult to identify for sufficiently boosted π^0 mesons; in this case, the two photons are confined to a small enough solid angle that the cluster reconstruction software may only identify a single merged photon cluster. The magnitude of this background in the sPHENIX forward electromagnetic calorimeter is discussed, and the regions for which it is most and least significant are characterized. Possible improvements for correctly identifying this decay and thus further improving statistics for direct photon measurements are also suggested.

Dedication

This document is dedicated to my family, friends, and colleagues who have contributed either significantly or in part to the success which this document symbolizes to me. Thank you for all the help, encouragement, and support throughout the years, without which this work would not have been realized.

Declaration

I hereby declare that I am the sole author of this undergraduate honors thesis, submitted to the University of Michigan Physics Department in the College of Literature, Science, and the Arts for the partial completion of the requirements for the degree of Bachelor of Science in Physics with Honors.

I authorize the University of Michigan to lend this undergraduate honors thesis to other institutions or individuals for the purpose of scholarly research.

Ezra D. Lesser, March 11, 2018

I further authorize the University of Michigan to reproduce this undergraduate honors thesis by photocopying or by other means, in total or in part, at the request of other institutions or individuals for the purpose of scholarly research.

Ezra D. Lesser, March 11, 2018

Acknowledgments

I would foremost like to thank Professor Christine A. Aidala for her continual altruistic guidance throughout my college career and for all of the opportunities which she has offered since my second semester the University of Michigan. Having the chance to work with Professor Aidala's group both introduced me to the fields of experimental nuclear and particle physics as well as illuminated my interests in electronics and instrumentation, nuclear and hadronic structure, and quantum chromodynamics. I could not have asked for a more perfect research environment, for a more helpful advisor, or for a stronger group dynamic than in Professor Aidala's group. This document certainly would not have been possible without her support.

I would also like to thank PhD candidate Joseph D. Osborn, who spent numerous hours explaining the fundamentals of the sPHENIX software framework to me after I switched efforts to this collaboration. Joe guided numerous discussions on physics and analysis and answered many questions which became invaluable and greatly contributed to the work that I completed. His help, which sometimes was even at odd hours of the night, made this study and document possible.

Contents

List of Figures

Chapter 1

Introduction

The currently-accepted understanding of physical interactions is broken into four fundamental forces which are by definition not reducible to more basic forms or forces. One of these four fundamental interactions is known as the *strong force*, so-named as it has the greatest relative strength. The strong force is responsible both for binding partons into hadrons (called the *fundamental strong force*, mediated by gluons) and for holding nucleons together inside atomic nuclei (called the *residual strong force*, mediated by π, ρ, and ω mesons).

Quantum chromodynamics (QCD) is the current theoretical model that describes the strong interaction. In QCD there are numerous open questions which are areas of active research today [Aidala et al. 2013]. Unlike the electromagnetic force, which has only two opposite charges of one type, QCD elucidates that the strong force has three distinct types of charge. The electroweak theory, which unifies the electromagnetic interaction and the weak nuclear force into the *electroweak force*, describes the unified electroweak interaction as mediated by γ, Z, and W bosons. While photons have no electric charge, W bosons do, and both Z and W mediators carry weak charge. Comparably, gluons (which mediate the strong force) carry charge in the strong interaction, although this is somewhat complicated in QCD physics as explained below.

The three charges in QCD are referred to as *color*, borrowing terminology from the orthogonal basis of red, green, and blue colors perceived by human eye cones [Fritzsch, Gell-Mann, and Leutwyler 1973]. This naming scheme, however, has no direct relation to the optical meaning in any other sense [Feynman 1985, p. 136]. Since all particles have corresponding antiparticles, for color to be conserved under particle-antiparticle annihilation, the corresponding charge for antiparticles must be anticolor (antired, antigreen, and antiblue). Color and anticolor are analogous to the opposite positive and negative charges in classical electromagnetism.

Particles that have color charge are currently understood by a theoretical presentation referred to as the *standard model of particle physics*. This theory suggests in part that the universe is composed from 17 irreducible particles along with their fundamental interactions. These particles, and some of their innate properties, are depicted in Figure 1.1.

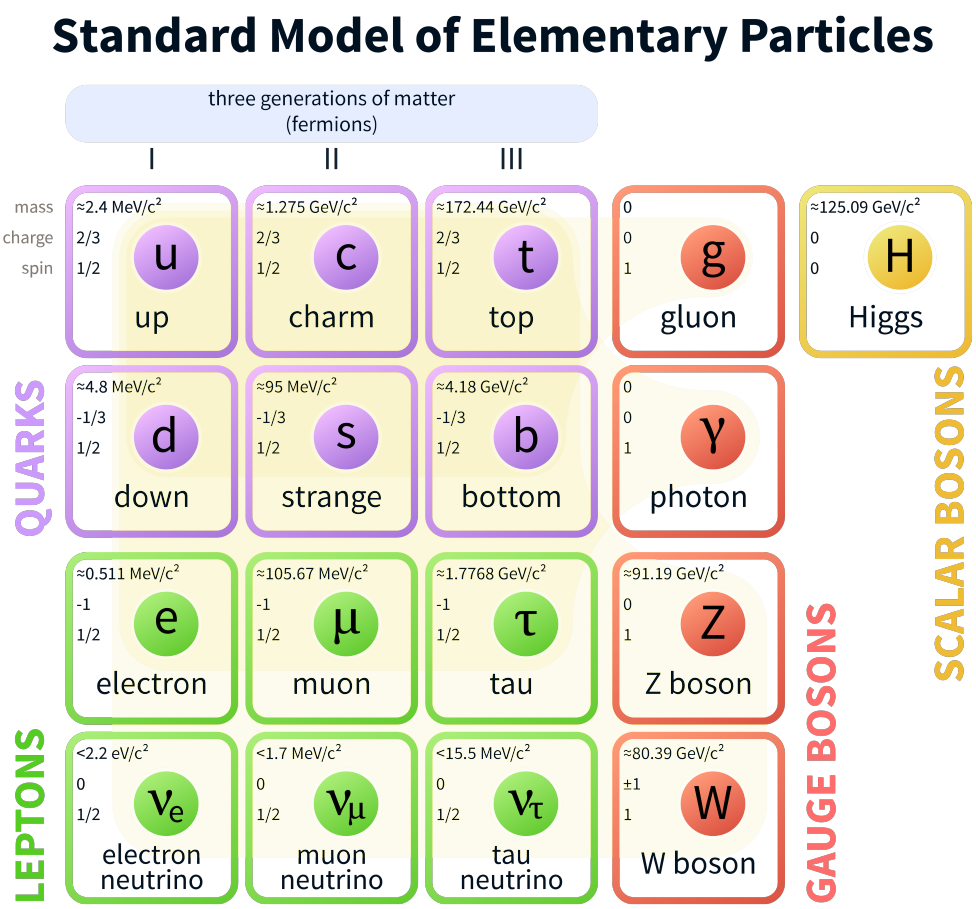

Figure 1.1: Standard model of particle physics, depicting in part the gluon and six quarks relevant in QCD [Wikimedia Commons 2006].

Together with the gluon gauge boson, the six quarks in this model constitute a particle class known as *partons*. These were first proposed and named in 1969 by American theoretical physicist Richard Feynman as an answer to the "parts" that compose some heavier bound-states known as *hadrons*. The leptons, neutrinos, and other three gauge bosons interact via the electroweak force, while the Higgs (the only experimentally detected scalar boson) is what gives other particles their mass. Only partons are color-charged, with quarks having one color and gluons having a combination of a color and an anticolor, thus these are the interests of QCD studies.

In the electromagnetic interaction, the mediating γ gauge boson has no charge; in the weak interaction, the W and Z bosons which carry weak charge are so massive that the weak force cannot form bound states. Gluons contradictorily carry color (in eight possible states) and are theoretically massless, complicating experimental analysis of coupling interactions. This non-Abelian nature also leads to a larger set of possible *Feynman diagrams*, or pictorial representations of available subatomic interactions. The W boson carries electric charge, but the effect is less prominent than in QCD due to the smaller coupling constant $\alpha_{EM} < \alpha_S$,

and while the W and Z carry weak charge, the weak coupling is in turn even weaker than the electromagnetic coupling.

Also unlike the electroweak force, studies of the strong interaction are further complicated by *confinement*. This is the phenomenon that, at the length scale of nucleons or at energy scales less than about 1 GeV, partons are confined to color-neutral bound states with other partons [Greensite 2011]. However, a property called *asymptotic freedom* changes confinement properties at higher interaction energies. As particle energy increases and the corresponding length scale decreases, QCD dictates that the strong force becomes asymptotically weaker [Gross and Wilczek 1973, Politzer 1973]. At energy scales corresponding to a momentum transfer Q on the order of several GeV, color-charged particles can be directly probed via deep inelastic scattering.

At these high temperatures and/or densities, nuclear collisions created by particle accelerators allow quarks and gluons to form a new state of matter called the quark-gluon plasma (QGP). This phase of matter is formed at the Hagedorn temperature, which corresponds to about 2×10^{12} K (or energies of approximately 130-140 MeV per particle) [Barger and Phillips 1997]. The QGP can be created and thus studied at facilities such as the Relativistic Heavy Ion Collider (RHIC) at Brookhaven National Lab (BNL) in Upton, New York, USA, or the Large Hadron Collider (LHC) at the European Center for Nuclear Research (CERN) on the Franco-Swiss border near Geneva, Switzerland. However, the QGP is unstable and difficult to contain, and it cools down to form stable particles via hadronization within a fraction of a second after creation [Bohr and Nielsen 1977]. Proton-proton collisions are not used

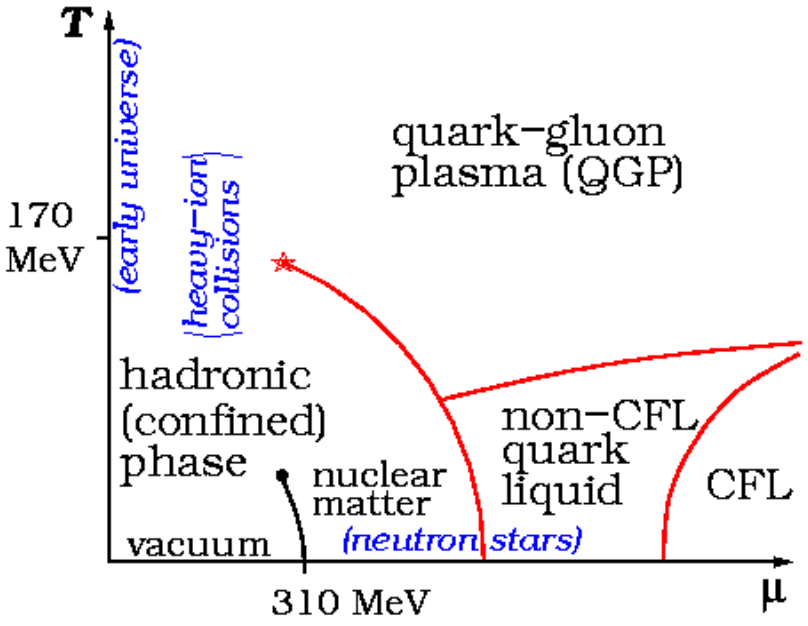

Figure 1.2: Conjectured phases of nuclear matter with respect to temperature and density, showing the predicted regime of quark-gluon plasma (QGP) and color-flavor-locked (CFL) matter. [Wikimedia Commons 2011].

to create the QGP since the energy density is lower than that of nucleus-nucleus collisions. A relative energy diagram of quark matter is given in Figure 1.2, where the quark-gluon plasma is shown at high temperatures T and densities. This figure also shows the theoretical prediction of a color-flavor-locked (CFL) phase of color-superconducting quark matter at higher chemical potential μ [Alford et al. 2008]. Contrarily, at low T and μ, partons are confined to hadrons.

Besides interest in the basic physical properties of QGP, studying these extremely high-temperature states is essential to understanding the quark epoch that began approximately 10^{-12} s after the big bang [Allday 2002]. Studying the QGP could reveal hints as to why the observable universe is made up of primarily matter as opposed to the predicted model of equal amounts matter and antimatter, which would instead lead to a radiation-dominated universe. This question is therefore seen as an important query into "big picture" ideas such as the origin of the universe and the existence of life.

QGP studies can also be used as a direct test of QCD and measurement of its nonperturbative effects. The particles that hadronize out of the QGP allow a direct probe for the decoupled interactions between quarks and gluons. One interaction of particular interest is the creation and emission of a direct photon from a hard scattering process, as shown above in Figure 1.3a. The resulting photon from this process is of particular interest to experimentalists since photons are experimentally easy to measure and thus correlate strongly to the initial partonic interaction. Due to confinement, however, quarks and gluons first hadronize before detection into strongly correlated bunches of particles called jets. The measurement of jets provides useful information on the QGP interactions but are experimentally more difficult to measure with the same accuracy as direct photons due to the sheer amount of final-state particles and detector inefficiencies. Also, direct photons are unaffected by color interactions, unlike hard-scattered quarks or gluons that form modified jets after losing energy in the QGP. Jets are nonetheless invaluable as they also provide insight into the discovery of new particles predicted by the standard model; the Higgs boson was confirmed by the ATLAS and CMS collaborations in 2012 [*The Nobel Prize in Physics 2013* 2014] via

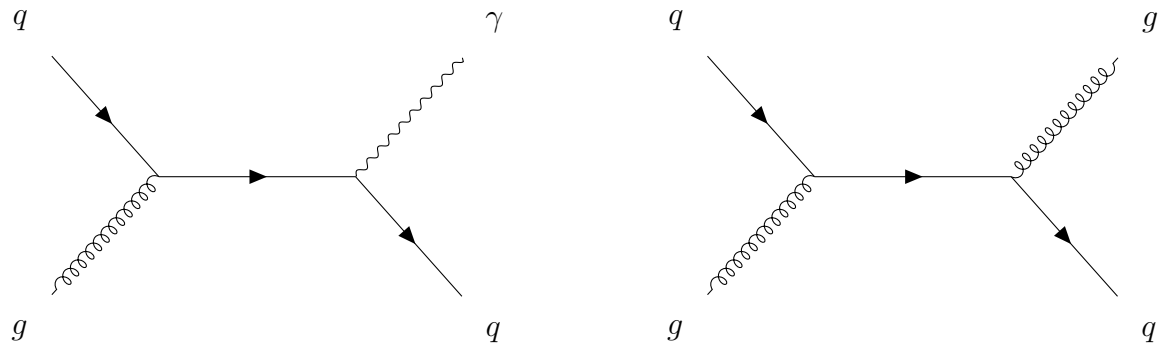

(a) Emission of a direct photon from hard quark-gluon interaction.

(b) Interaction of a quark and gluon which allows rotation in color and energy space.

Figure 1.3: Two possible Feynman diagrams for hard-scale interactions.

$H \to ZZ \to 4l$ and $H \to \gamma\gamma$ and has since been found via particle jets [Carpenter et al. 2017].

However, direct photons can be obscured by other processes occurring during and after hadron freeze-out. Jets can in general include photons either from hadron decays or from radiative processes involving the jet products. The jet produced during hadronization from the quark in the direct photon process is separated from the direct photon in space due to conservation of momentum in the lab frame, but Figure 1.3b depicts another process which can more directly contribute to photon background via hadron decays. This interaction is also more common than direct photon emission since the strong force has greater strength than the electromagnetic interaction ($\frac{1}{\alpha_{EM}} \approx \frac{1}{137}$ versus $\alpha_S \approx 0.1$).

One of the predominant ways in which a jet can produce photonic background is via decay of neutral pions into two photons which are back-to-back in the initial π^0 rest frame:

$$\pi^0 \to \gamma\gamma$$

which occurs about 8.4×10^{-17} s after creation of the π^0. However, since particles in jets have very high momentum in the lab frame, these photons which are back-to-back in the initial π^0 rest frame are very boosted in the lab frame and will hit the detector within a reasonably small solid angle. Being able to differentiate between one photon and two depends significantly on detector resolution and reconstruction algorithms. For that reason, hardware and software design necessitates careful attention to the required spatial resolution for correct reconstruction of these two photons. If the detector resolution is poor or software does not adequately address this issue, the two photons could appear as a single particle after reconstruction, effectively merging their information into something that masquerades as a single direct photon emitted from the hard-scale process.

For sufficiently energetic photons ($E > 2m_e c^2 \approx 1.022\,\text{MeV}$) it is also possible to decay into an electron and positron via pair creation:

$$\pi^0 \to \gamma + e^- + e^+$$

which is called the Dalitz decay after Australian particle physicist Richard Dalitz. This process requires correct reconstruction of not only the photon but also both the electron and positron pair for correct identification. However, this process is not the predominant background from neutral pions since it occurs only about 1.2% of the time. Double Dalitz decay, where the π^0 instead decays into two positron-electron pairs, is also possible but only occurs about 3×10^{-3} % of the time.

An important goal, then, is to understand the effect of $\pi^0 \to \gamma\gamma$ as a background for direct photons and characterize for which conditions merging occurs in the detector. In forward rapidities where particles are very boosted, the probability of two photon clusters merging is greater, and so it is especially important to understand these characteristics for proper statistics and background subtraction.

Chapter 2

Overview of sPHENIX

2.1 Introduction to sPHENIX

sPHENIX, acronymically meaning "super PHENIX," is an experiment proposed as the successor to PHENIX, the Pioneering High Energy Nuclear Interaction eXperiment, located at RHIC. Although PHENIX finished taking data in 2016, the sPHENIX collaboration will continue nuclear interaction studies with a refreshed physics interest. sPHENIX will use the 1.5 T superconducting magnetic solenoid developed for the BaBar experiment at SLAC National Accelerator Laboratory [Adare et al. 2015]. It will also integrate electromagnetic and hadronic calorimetry providing uniform coverage for psuedorapidity $|\eta| < 1$ and instrumentation for tracking and detecting particles at very forward rapidity ($1.4 < \eta < 4$) including refurbished components from the PHENIX electromagnetic calorimeter. A diagram is given in Figure 2.1.

sPHENIX has the primary physics goal of investigating strongly-interacting particles in

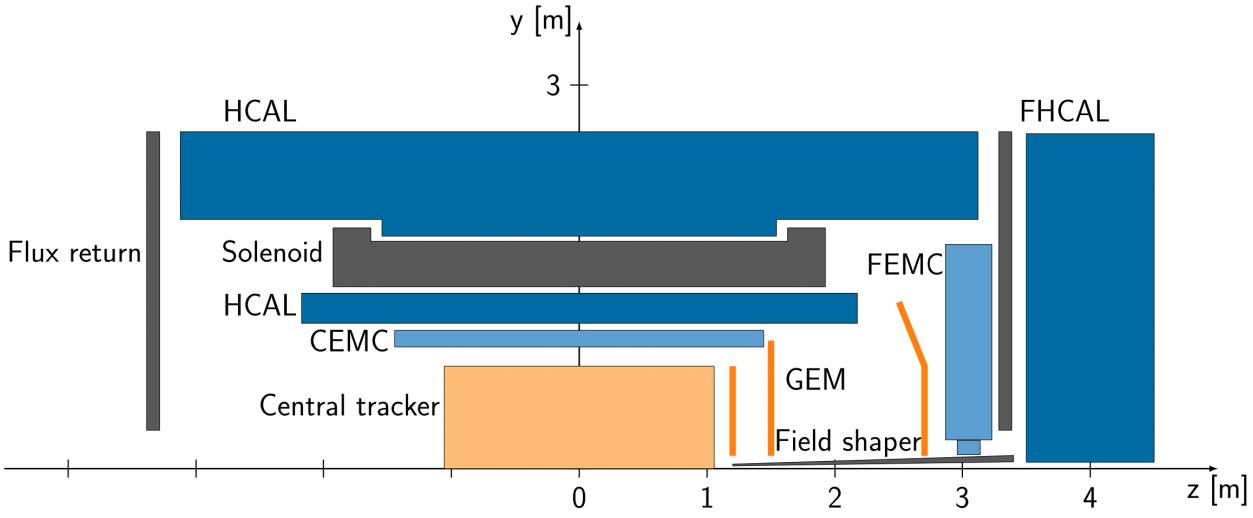

Figure 2.1: Cross-section of sPHENIX detector with proposed forward instrumentation (GEM, FEMC, and FHCAL) [sPHENIX collaboration 2017].

the QGP via jets and heavy-flavor observables that result from the collisions of both protons and heavy ions [sPHENIX Collaboration 2018]. Over a 20-week run, sPHENIX will be able to measure 10^{12} gold-on-gold (Au+Au) collisions and have mass resolution capable of distinguishing the three upsilon mesons (Υ(1S), Υ(2S), and Υ(3S)). These particles are different energy states of a bottom-antibottom quark pair that can decay into a lepton-antilepton pair ($\Upsilon(\mathrm{nS}) \to e^+e^-$ for example) [Particle Data Group 2016]. Heavy-flavor mesons such as the upsilon and J/ψ (composed from a charm-anticharm pair) are of particular interest since their constituent quarks have relatively high mass and thus their dynamics in the QGP make them excellent experimental probes [Liboff 2011].

The energy scale of the heavy ion collisions is directly related to the length scale of the QGP being probed. At the higher energy collisions which are achieved at the LHC (and primarily use Pb+Pb species at these higher center of mass energies), jets can be reliably measured down to 40 GeV [Adare et al. 2015], which is well within the scale of sPHENIX reconstructions; however, the lower energy collisions produced at RHIC will provide a measurement of larger distance scales as well as different temperatures and coupling strengths of the QGP [Adare et al. 2015].

2.1.1 Forward instrumentation

The proposed sPHENIX forward instrumentation is composed of three gas-electron multiplier (GEM) stations, a lead-scintillator electromagnetic calorimeter (EMC) at intermediate pseudorapidities with a lead-tungstate crystal electromagnetic calorimeter at high pseudorapidities (forward EMC or FEMC), a steel-scintillator hadron calorimeter (forward HCAL or FHCAL), and a field shaping steel piston [sPHENIX collaboration 2017] which are depicted in Figure 2.1. The primary goal of the added instrumentation is providing a new channel to study the formation, interactions, structure and properties of QCD systems, as discussed above. For studying the $\pi^0 \to \gamma\gamma$ process of interest in this document, the most important component of this setup is the FEMC, as photons have no charge but interact electromagnetically in the EMC volume via the photoelectric effect, Compton scattering, and particle-antiparticle pair production.

The three GEM detectors are placed within 3 m of the interaction point (IP) where collisions occur. These intermediate stations provide excellent tracking and momentum determination for charged particles, but they may also provide an interface for interaction via the three mechanisms mentioned above. For this reason, their effects cannot be ignored in simulation or during characterization of expected background. The same is true for the field shaper, even though this element is at a high pseudorapidity and not in the direct path of the calorimetry.

Electrons and photons at forward rapidities in the sPHENIX detector will be measured via the FEMC, which will also help in measuring jets. Both regions, the lead-scintillator (PbSc) portion ($1.4 < \eta < 3 - 3.3$) and the lead-tungstate ($PbWO_4$) portion ($3 - 3.3 < \eta < 4$), will be refurbished from existing PHENIX materials shown in Figure 2.2. Scintillation light

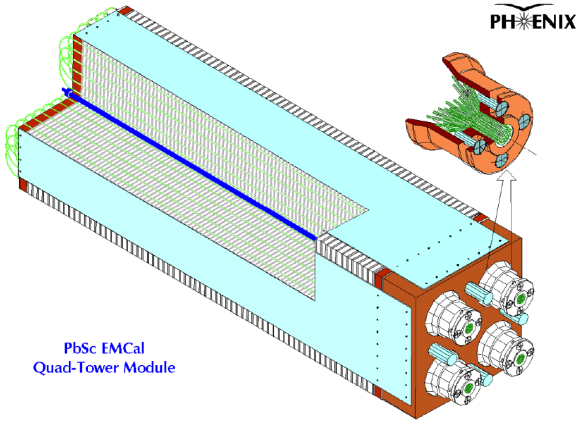

(a) PbSc tower of size 5.5 x 5.5 cm^2 and energy resolution of $\sigma_E/E \approx 8\%/\sqrt{E(GeV)}$.

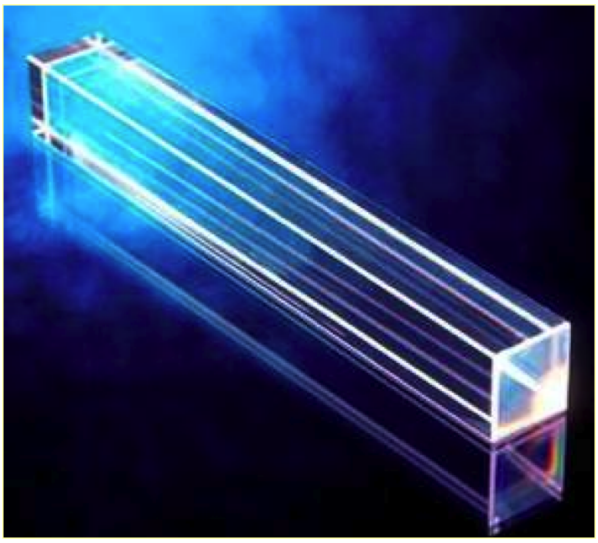

(b) $PbWO_4$ tower of size 2.2 x 2.2 cm^2 and energy resolution of $\sigma_E/E \approx 12\%/\sqrt{E(GeV)}$.

Figure 2.2: FEMC towers to be reused from PHENIX [sPHENIX collaboration 2017].

will be read out via silicon photomultipliers (SiPMs) which have a relatively low cost and are much smaller than photomultiplier tubes (PMTs), and are able to operate inside of magnetic fields.

2.2 sPHENIX simulation framework

Simulations for sPHENIX are performed within a core software framework called Fun4All. This system was originally developed in 2002 for PHENIX and is based around an underlying data structure referred to as the PHENIX node tree. The main goal of Fun4All was to allow for various analysis and reconstruction needs to be developed independently by different users within a single system [Pinkenburg 2015].

Initial particle and detector simulations are performed using the GEANT4 toolkit maintained by CERN. GEANT4 generates simulations using a Monte Carlo method, meaning that the software relies on repeated random samplings of a large database of physical data in order to generate numerical results. This software also allows for careful simulated construction of the sPHENIX detector and permits the user to fine-tune the detector conditions in order to characterize sPHENIX and similar detectors in high energy physics (HEP). The output data from GEANT4 is directly ported into the Fun4All framework, where an analysis package can be written to obtain and save the meaningful data. Fun4All also allows for data to be read from various other formats, including PHENIX raw data (PRDF), PHENIX data summary tape (DST), the Oscar data format, and HepMC event records from other Monte Carlo generators.

The data from Fun4All can then be ported into various software packages for physics

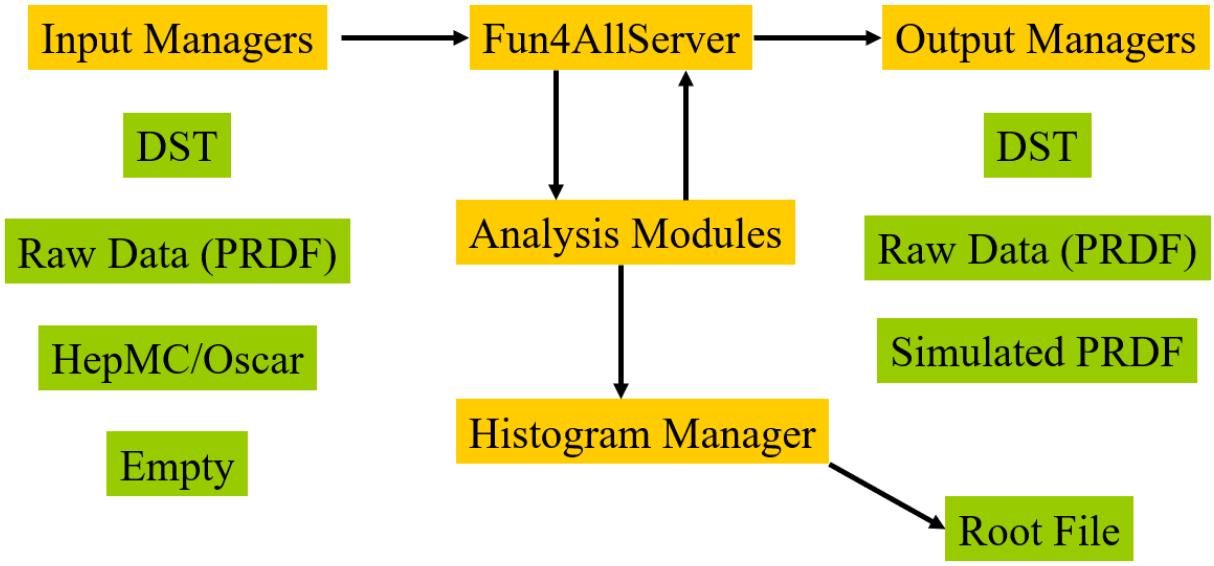

Figure 2.3: Data workflow for the Fun4All software framework [Pinkenburg 2015].

analysis. These programs analyze the input data and can create data structures to be stored in the industry-standard ROOT format. ROOT is a modular scientific software framework also maintained by CERN that boasts functionalities needed to deal with big data processing, statistical analysis, visualisation and storage [CERN n.d.]. Simulations for single photons and neutral pions can be analyzed using the sPHENIX PhotonJet package, written by sPHENIX collaborator Joseph Osborn. This analysis package outputs single ROOT files per simulation containing custom-filled *TTrees*, a ROOT data object containing a header and a list of independent *TBranches* which themselves hold individual data objects as *TLeaves*. Utilizing this data, ROOT macros can be written in object-oriented C++ for further analysis of generated data. A diagram detailing the Fun4All data workflow is given in Figure 2.3.

2.2.1 Cluster Computing with Condor

Physics simulations with GEANT4 can be quite computationally challenging. In addition to simulating the correct material properties and dimensions of all sPHENIX hardware components, the particles thrown for each event must obey known quantum probabilistic principles at each moment of their trajectory, including decays and interactions with other simulated objects. The simulation of single events can take from a handful of minutes to significant fractions of an hour, depending on the type of process being studied. The number of events required for meaningful statistical analysis, however, can be on the order of thousands, or even hundreds of thousands, as was required for the study described in this document.

For this reason, it is useful to distribute the task of calculating these computations across numerous computers running in parallel and then assemble the results. This is the basic con-

cept of distributed computing and is accomplished at the RHIC Computing Facility (RCF) through Condor. This system allows batch queuing and scheduling jobs between various users while maintaining a policy-driven resource allocation control to help ensure optimal performance [RACF 2014].

For the purpose of this experiment, Condor was used to submit computational jobs to hundreds of nodes based on the servers at RCF. Using this parallel technology and distributive algorithm, individual simulations with reasonable statistics were capable of being completed on the timescale of only one or two days, as compared to the weeks or months that a single thread would take to process and create this volume of data.

Chapter 3

Simulation Results

3.1 Single Photons

Before considering the relatively complicated effects that can arise from the detection of neutral pion decay products, it is beneficial to first consider single photons, thrown in the forward region of sPHENIX that is of interest. For this analysis, single photons were thrown uniformly between $1.4 < \eta < 3.0$, which is exactly the psuedorapidity range of the PbSc portion of the sPHENIX FEMC. The photons were also generated uniformly in the momentum space $2 < p < 20$ GeV/c with respect to the lab frame. This momentum range was picked since photons below 2 GeV/c are generally not of physical interest, while photons above 20 GeV are relatively rare due to RHIC collision energies. In order to provide sufficient statistics, the simulation was run for roughly 500 000 events.

In addition to providing data to juxtapose with forward clusters from photons that come from neutral pion decays, throwing single photons is important for characterizing what an ideal signal of direct photons would look like in the sPHENIX forward instrumentation. This data, as described previously, is a major signal of interest due to its direct correlation to the hard-scale interactions that arise in the initial collision, and thus it is useful to quantitatively describe and understand what the characteristics of this signal should be.

One such quantity is the *energy response*, as depicted in Figure 3.1. This value is calculated by dividing the reconstructed cluster energy by the known initial truth energy generated by the simulation. An ideal detector would have this number equal to 1 for all events, but detector inefficiencies limit the actual energy response of real experiments. One such inefficiency for the sPHENIX FEMC is the tower structure, or specifically the necessity for a boundary between scintillator towers. If a particle interacts with and loses all of its energy in the central region of a scintillator, then its energy can ideally be reconstructed such that the response is very near to 1. If the particle interacts with the region very close to or in the boundary between the scintillating tiles, however, some energy will be lost, lowering the expected response. This effect, along with others and the inherent properties of detector statistics, leads to some variation in both the spectrum's mean and width. This width is called the *energy resolution*, whereas the mean energy response is called the *energy scale*.

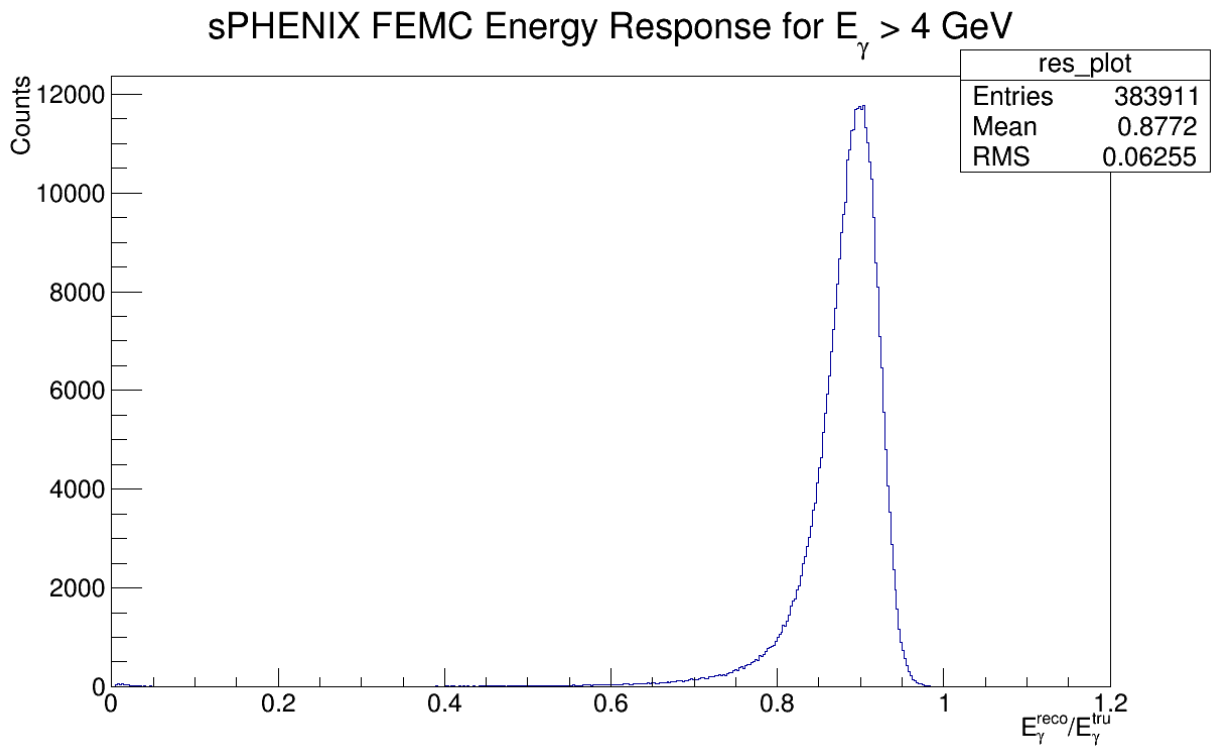

Figure 3.1: Energy response plot for single forward photons in the FEMC ($1.4 < \eta < 3$).

Figure 3.1 also has an energy cut to maintain only events $E_\gamma > 4\,\text{GeV}$; this is because the energy response is strongly nonlinear at lower energies. However, the energy resolution spectrum can be approximated as linear (to within approximately 1%) in the higher energy regime. Energy scale and resolution plots for the same FEMC simulation are given in Figures 3.2 and 3.3.

3.1.1 Resolution of η and ϕ

The relative simplicity of single forward photon simulations also permits characterization of FEMC sensitivity to both photon psuedorapidity η and azimuthal angle ϕ. This property can be examined by considering both the relative cluster-to-truth spectra and the residuals between cluster and truth values. These plots are given in Figures 3.4 and 3.5 for ϕ and η, respectively.

Using the width of the resolution plots for η and ϕ from these figures, we can begin to develop an algorithm for determining if a given cluster for an event is likely to be from the expected photon or if it is more likely to be either from alternate particles created via pair production or interaction with detector materials or from other background noise sources. The calculated width from a Gaussian fit to these distributions is given in Table 3.1. The Gaussian fits are used as an approximation to understand the core azimuthal and pseudorapidity resolution of the towers. The η resolution plot also has a slightly shifted

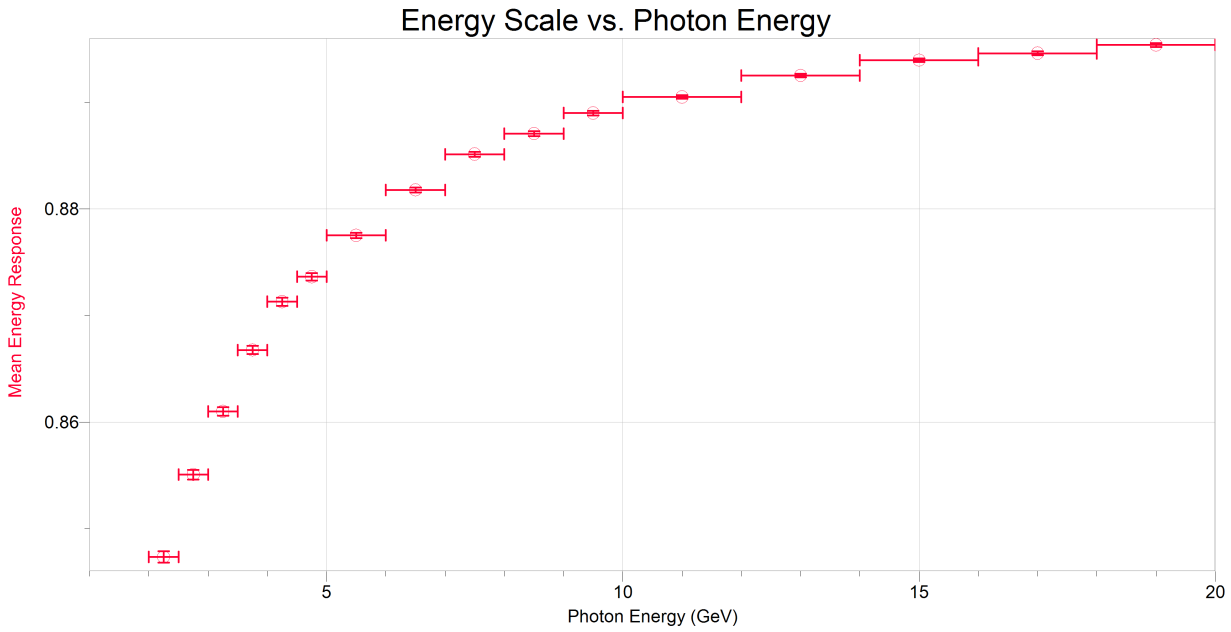

Figure 3.2: Plot showing the shift in energy scale with respect to different photon energy ranges in the sPHENIX FEMC.

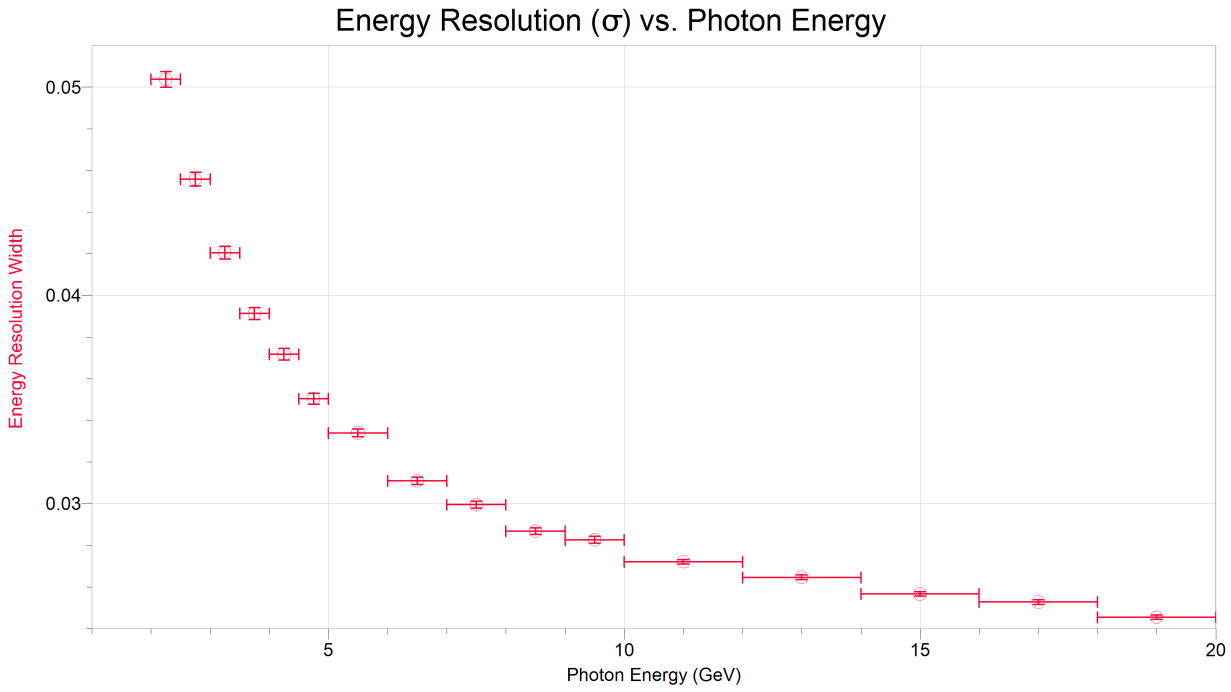

Figure 3.3: Plot showing the shift in energy resolution (σ) with respect to different photon energy ranges in the sPHENIX FEMC.

nonzero mean of -0.00508 ± 0.00003 due to incident photons traversing multiple towers.

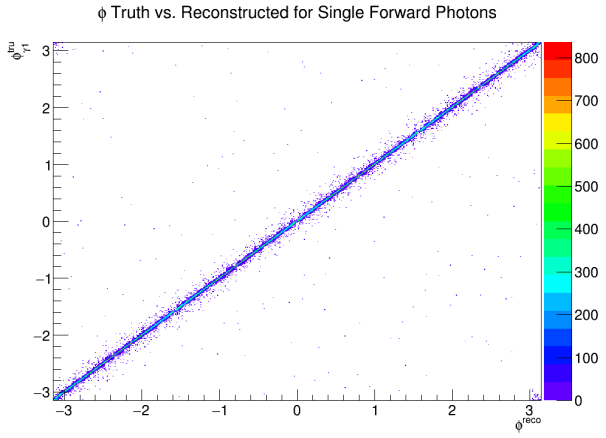

(a) Truth versus reconstructed ϕ for single forward photons.

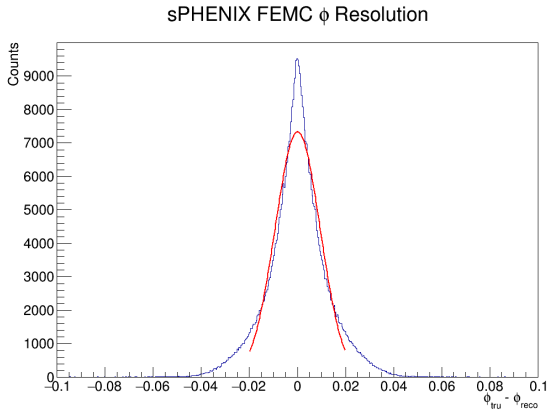

(b) Spectrum of ϕ truth-minus-reco for single forward photons (blue) with Gaussian fit (red).

Figure 3.4: Resolution of azimuthal angle ϕ in the proposed sPHENIX FEMC for single forward photons.

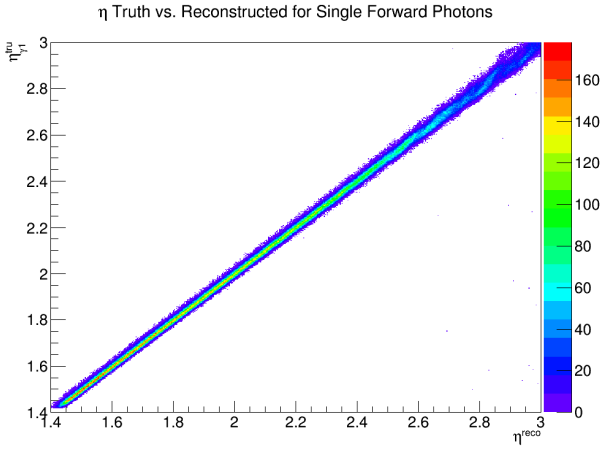

(a) Truth versus reconstructed η for single forward photons.

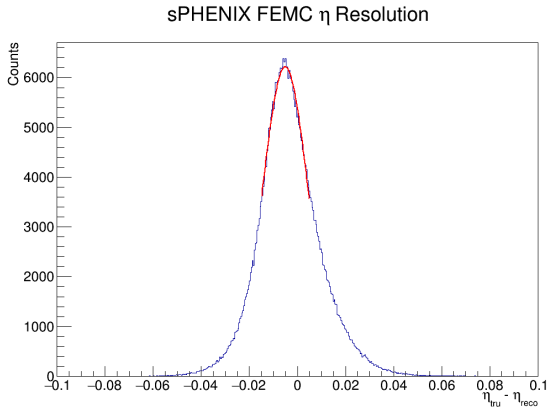

(b) Spectrum of η truth-minus-reco for single forward photons (blue) with Gaussian fit (red).

Figure 3.5: Resolution of psuedorapidity η in the proposed sPHENIX FEMC for single forward photons.

Parameter	σ	Error
ϕ	0.00938	0.000018
η	0.00947	0.000059

Table 3.1: Gaussian widths for the resolution plots given in Figures 3.4b and 3.5b.

3.2 Forward-Rapidity $\pi^0 \to \gamma\gamma$ Analysis

The main region of interest for this study is in the proposed sPHENIX forward instrumentation, specifically in the region $1.4 < \eta < 3$ where the PbSc towers of the FEMC are located. Since the π^0 mesons in this region are in general very boosted, their decay products, which are confined to a small solid angle, are more difficult to ensure proper discrete reconstruction.

All the neutrally-charged pions are expected to decay before having the opportunity to interact with any detector components, since the mean lifetime of the particle is so short; therefore, all π^0 mesons must be reconstructed by their decay products, primarily photons, which create clusters of energy in the FEMC. By doing a simulation of single forward π^0 mesons, it is possible then to analyze the simulated data much like that of single forward photons. A simulation was done for 500 000 neutral pions thrown in the region of interest, again randomly in the range $2 < p < 20$ GeV/c. An energy response plot was created as an analog to Figure 3.1, which is given in Figure 3.6. However, this plot shows a slightly different structure to the comparable single photon analysis.

Figure 3.6 shows, in addition to the expected peak structure from before, a significant additional tail for energy response $E_{reco}/E_{tru} > 0.94$ which skews the spectrum to the right. An important question, then, is how the photons that are created from π^0 decay can exhibit this different behavior as compared to simulated single photons. This effect is from the merging of photon clusters which are closely related in space during reconstruction. If two photons are reconstructed in a single cluster, this sums their energies, accounting for a greater energy than physically possible from either of the individual photons.

To test this hypothesis, an algorithm was created to help discriminate clusters and count

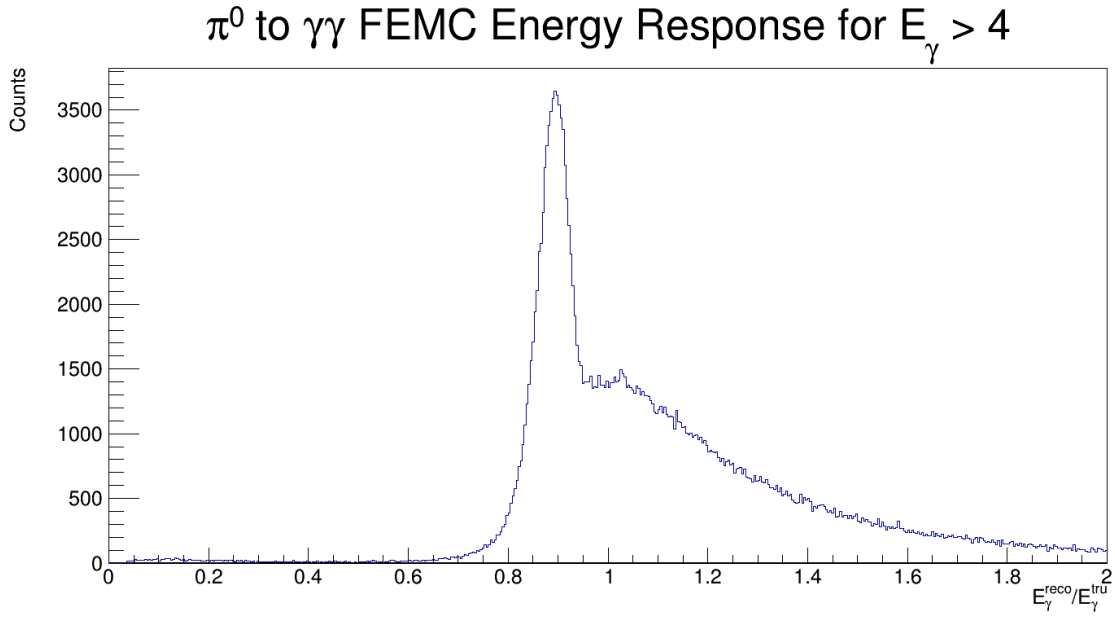

Figure 3.6: Cluster energy response in the FEMC ($1.4 < \eta < 3$) for single π^0 mesons.

the number of photonic-looking clusters per event. Clusters were separated into categories of 'good' and 'bad' by selecting on a number of variables:

1. The event must correspond to only $\pi^0 \to \gamma\gamma$ decay (this is to exclude Dalitz and double-Dalitz decays from inclusion);

2. Both photons must have interacted within FEMC ($1.4 < \eta < 3$);

3. Photons must have high enough energy to approximately linearize resolution ($E_\gamma > 4$);

4. The cluster energy response must have $E_{reco}/E_{tru} > 0.5$ for the appropriate truth photon information; and

5. Clusters must be within a small $\Delta\phi < 0.02$ of initial photon azimuthal angle.

where only clusters that all of satisfy the given requirements are 'good,' and all others are 'bad.' The reason for the final cut on ϕ is that the detector is known to have a resolution of ϕ and η as given in Table 3.1, and using this cut can help exclude noise from photons that interact with alternate detector components and either change their trajectory or produce other particles.

While using this selection process, the algorithm linearly iterates through events and attempts to pair good clusters with other good clusters from the same event. This allows for the separation of events with good clusters into two subsets: events with only one 'good' photon cluster (labeled 1γ detection), and events with two (or more) 'good' photon clusters (labeled 2γ detection). Analysis can then be carried out on each subset individually. The energy response plots for these data subsets is given in Figure 3.7.

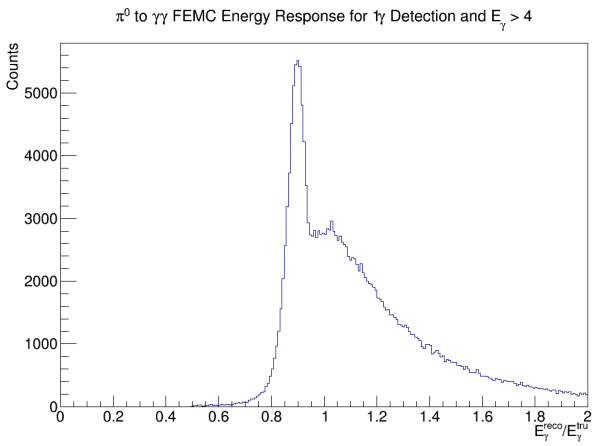

(a) Energy response for events with one 'good' cluster in the FEMC.

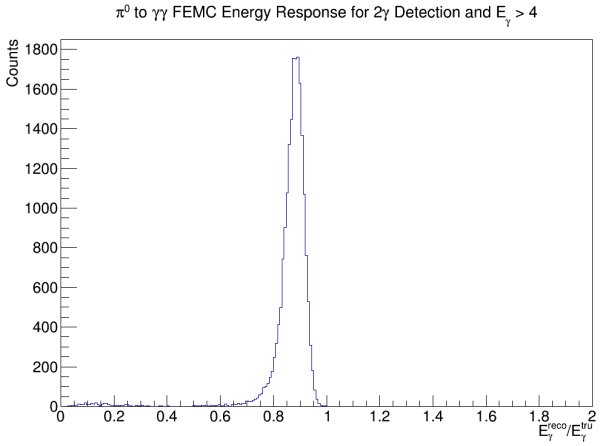

(b) Energy response for events with two 'good' clusters in the FEMC.

Figure 3.7: Cluster energy response in the sPHENIX FEMC for single forward π^0 mesons, separated into subsets of one-γ and two-γ cluster detections.

From these figures, it clear to see that the response spectrum for 2γ detection events closely resembles the expected single forward photon spectrum, whereas that of 1γ detection events contains a similar peak structure but also with the tail seen before. This helps explain the meaning of this structure: the 2γ detection plot looks similar to that for single forward photons since each photon from the π^0 decay is identified separately. However, merged clusters in the forward instrumentation prevent two individual photon clusters from being detected from the same event. Instead, a single cluster is reconstructed with energy from both individual photons.

3.2.1 Merging in p vs. η Spectrum

The next natural question to ask is for what neutral pion momentum this merging is most likely to occur. To answer this, it is useful to consider a plot of initial pion truth momentum versus pseudorapidity, as given in Figure 3.8. From examining the structure of these plots, it can be estimated that the maximum-efficiency region for correct reconstruction of forward π^0 mesons is from $1.5 < \eta < 2.5$ and $3 < p < 7$ GeV/c. For pions with $\eta < 1.5$ or $\eta > 2.9$, the spectrum has significant detector edge effects, meaning that it is likely for one photon to miss the detector completely; for $\eta > 2.5$, the decreasing detector resolution begins to limit two-photon reconstruction. Low-momentum π^0 mesons are more likely to have asymmetric decays leading to one or both photons missing the detector, while high-momentum π^0 mesons are more likely to have merged clusters from reconstruction. This is why the upper-left corner of Figure 3.8a is relatively dense, while the larger-p scales of Figure 3.8b are relatively sparse.

This method can be further validated by considering the relationship between the true initial π^0 energy and the energy of either the summed photon clusters (for 2γ detections) or single photon cluster (for 1γ detections). These relationships are shown in Figure 3.9. Both plots show a strong linear relationship, meaning that events with two distinct photon clusters

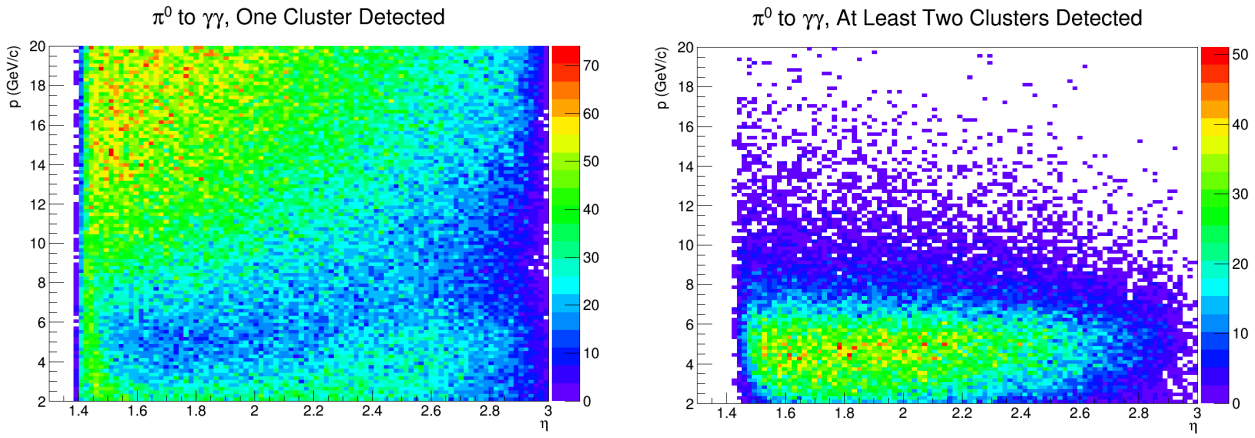

(a) Momentum versus η spectrum for events with one 'good' cluster in the FEMC.

(b) Momentum versus η spectrum for events with two 'good' clusters in the FEMC.

Figure 3.8: Momentum versus η spectrum for single forward π^0 mesons in the sPHENIX FEMC, separated into one-γ and two-γ cluster detections.

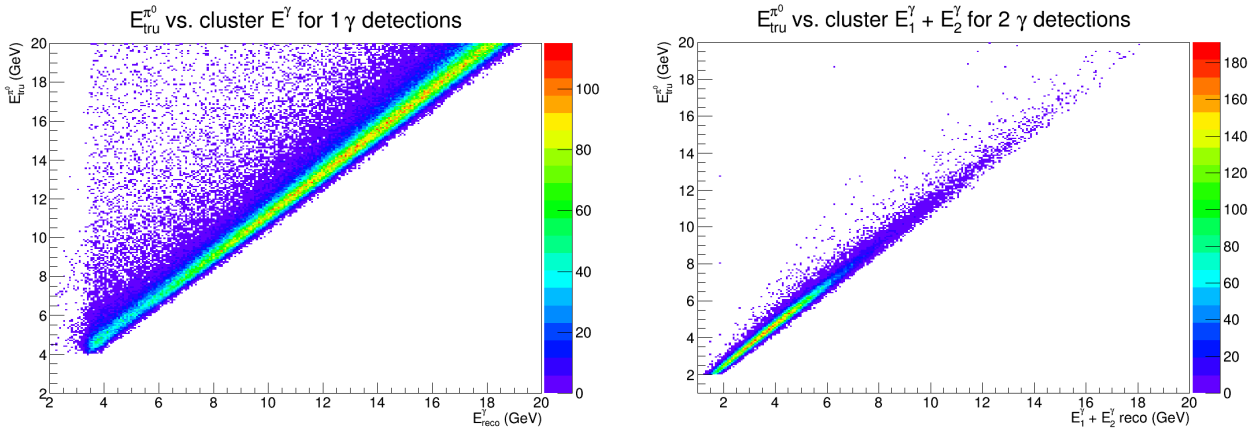

(a) Truth initial π^0 energy versus single cluster energy for events with one 'good' cluster in the FEMC.

(b) Truth initial π^0 energy versus summed cluster energies for events with two 'good' clusters in the FEMC.

Figure 3.9: Truth π^0 energy versus energy of the photonic cluster(s).

can be used to accurately determine the initial pion energy, but also helping prove that the events with single 'good' clusters are likely to contain clusters with two merged photons. The nonlinear points in Figure 3.9a are likely from asymmetric decays and detector edge effects, as discussed previously. Although important to consider, these effects are second-order processes at high enough pion energies.

3.2.2 Analysis in Mid-Region FEMC

By limiting the region of p and η space for which analysis is performed, it is possible to estimate the best possible efficiency of reconstruction of π^0 mesons in the FEMC. Approximate boundaries for this zoomed region should enclose the maximum number of correct reconstructions while minimizing the number of single-cluster events. Such a zoomed area is shown in Figure 3.10. By specifically considering the region $1.7 < \eta < 2.2$ and $3.5 < p < 6$ GeV/c, it is found that the best possible reconstruction efficiency of π^0 mesons from two-photon decays with the given detector geometry and clustering algorithm is approximately 62% in this region. This value is calculated by taking the number of 2γ detections and dividing by the total number of detections in that region.

Within this small subset region of the full detector, it is also possible to reanalyze the energy response to validate if minimizing high-p detections has the expected effect of reducing the right-hand-side tail structure for 1γ detections. The plotted results from this analysis, as shown in Figure 3.11, show that this structure indeed is reduced. This is because cutting out simulated data at higher momentum also cuts out a significant amount of merged clusters where $E^{\gamma}_{reco} > E^{\gamma}_{tru}$.

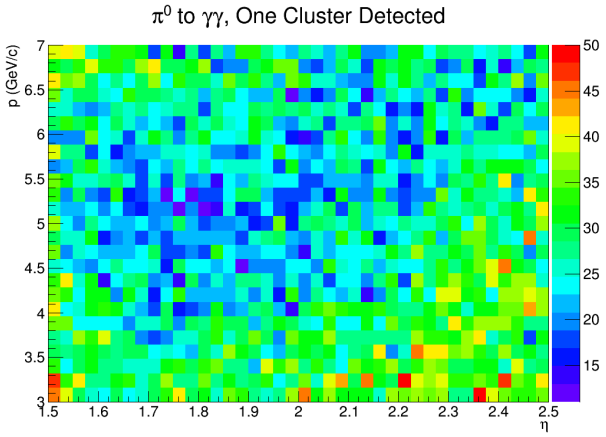

(a) Momentum versus η spectrum for events with one 'good' cluster in the mid-FEMC.

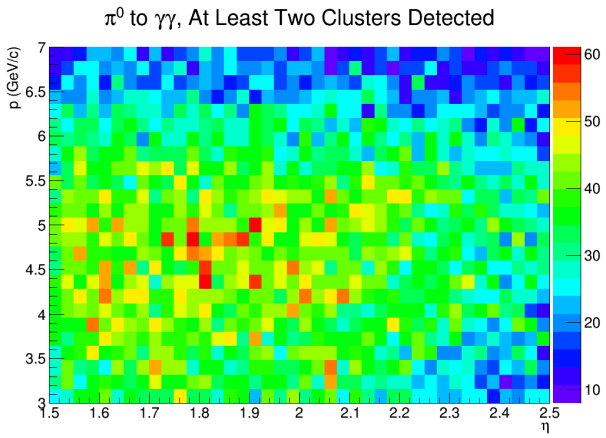

(b) Momentum versus η spectrum for events with two 'good' clusters in the mid-FEMC.

Figure 3.10: Momentum versus η spectrum for single forward π^0 mesons in the sPHENIX FEMC, separated into subsets of one-γ cluster detections and two-γ cluster detections, only considering a middle maximum-efficiency region.

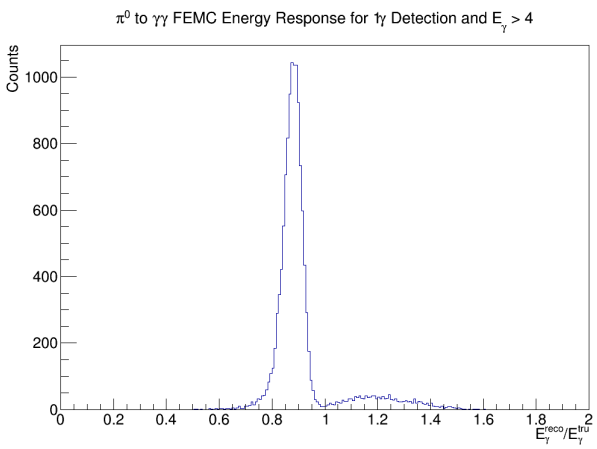

(a) Energy response for events with one 'good' cluster in the FEMC maximum-efficiency region.

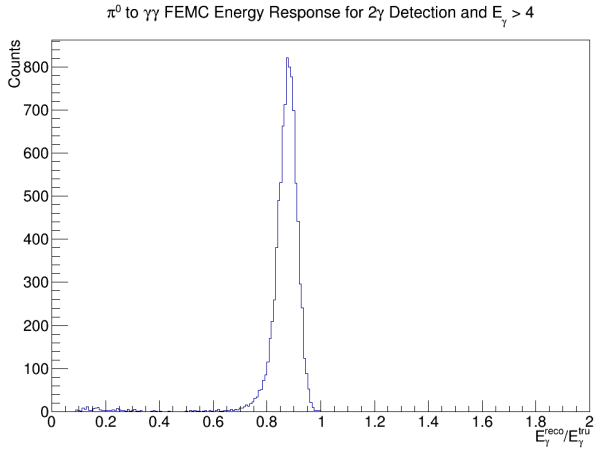

(b) Energy response for events with two 'good' clusters in the FEMC maximum-efficiency region.

Figure 3.11: Energy response for single π^0 mesons in the sPHENIX FEMC maximum-efficiency region, separated into one-γ and two-γ cluster detections.

Chapter 4

Conclusion

4.1 Summary

Studying direct photons from partonic hard scattering is an important tool for experimentally testing the theory of strong interactions, QCD. The information obtained from these studies will be essential for guiding theoretical discussions of the QGP as well as measuring spin asymmetries and factorization breaking. However, the relatively low strength of this direct photon signal as compared to jets that are emitted from parton scattering limits statistics in experiment. These backgrounds, such as the one arising from the $\pi^0 \rightarrow \gamma\gamma$ decay channel, must be properly characterized for proper statistical analysis of the direct photon signal.

The sPHENIX experiment at RHIC will permit new studies of these physics interests via collisions of both protons and heavy ions. The forward instrumentation, jointly composed of a GEM tracker, an EMCal, and a HCal, must be simulated properly to motivate physics measurements, inform detector construction, and hint at the challenges real data will have in future analysis. This study has shown that the sPHENIX FEMC may have sufficient resolution to identify direct photons with reasonable background statistics out to $\eta \approx 2.4$.

Neutral pions that decay into photons can most efficiently be reconstructed within the momentum-psudorapidity space of approximately $3 < p < 7$ GeV/c and $1.5 < \eta < 2.5$, with maximum efficiency around 62%, although this will likely be improved over the coming months (see Section 4.2 below). For momentum values $p > 7$ GeV/c, cluster merging becomes a predominant effect that limits reconstruction, while for psuedorapidity $\eta > 2.5$, detector resolution becomes too poor and limits sensitivity to 2γ detections. In the mid-region of the detector, merged clusters are much less likely, and 1γ detections are primarily due to asymmetric decays, gamma to particle-antiparticle pair production, Compton scattering within the GEM, Dalitz and double-Dalitz decays, and detector inefficiencies.

4.2 Improvements

The simulated reconstruction efficiency of 62% is less than what could probably be achieved with some future improvements to the software system. In general, the higher the accuracy with which π^0 mesons can be reconstructed, the lower the statistical background will be for direct photons, meaning that physical signals can be extracted with higher certainty from less data. In this context, it is important to reconstruct as many π^0 mesons as possible so that direct photons can be more easily observed. In real physics data where E_γ truth is not known, it is important to minimize as many effects perturbing the measured energy as possible.

The current best possible reconstruction efficiency is limited by the methodology used to draw boundaries between different clusters during reconstruction. This part of the software framework is referred to as the *clusterizer*. The default sPHENIX clusterizer is relatively basic and could benefit from algorithmic improvements. This is an area of active work within the sPHENIX collaboration, and algorithms have begun to be implemented. The efficiency of one such algorithm is shown in Figure 4.1. The efficiency with which neutral pions can be reconstructed via their two photon decays is approximately doubled for the new algorithm, suggesting that future software improvements could possibly extend the maximum-efficiency region of π^0 reconstruction up to around $p = 13\text{-}14$ GeV/c.

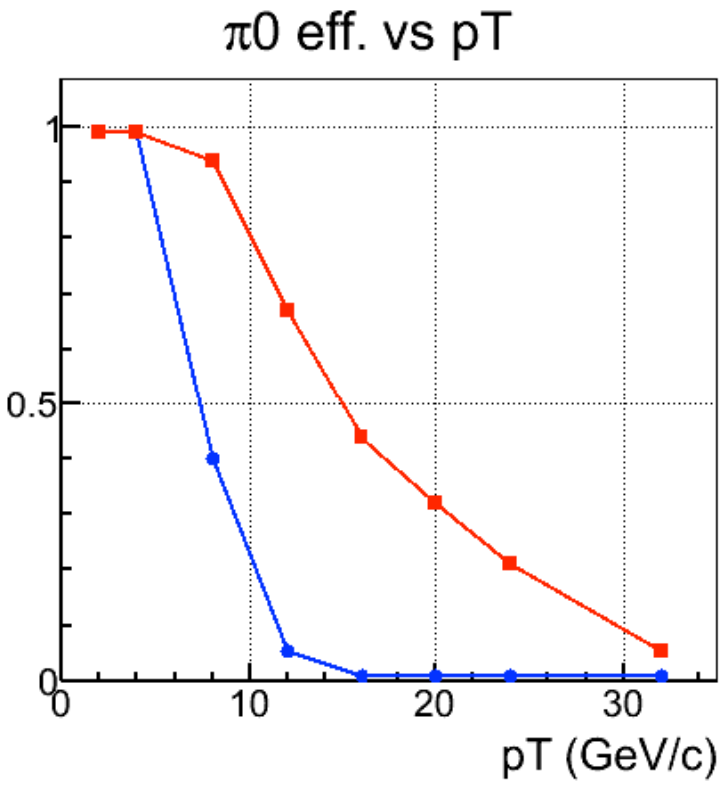

Figure 4.1: Measured π^0 reconstruction efficiency versus transverse momentum p_T for the new clusterizer (red) versus old (blue) [Bazilevsky 2017].

Bibliography

Aidala, Christine A. et al. (Apr. 2013). "The spin structure of the nucleon". In: *Rev. Mod. Phys.* 85 (2), pp. 655–691. DOI: 10.1103/RevModPhys.85.655. URL: https://link.aps.org/doi/10.1103/RevModPhys.85.655.

Fritzsch, H., M. Gell-Mann, and H. Leutwyler (1973). "Advantages of the color octet gluon picture". In: *Physics Letters B* 47.4, pp. 365–368. ISSN: 0370-2693. DOI: https://doi.org/10.1016/0370-2693(73)90625-4. URL: http://www.sciencedirect.com/science/article/pii/0370269373906254.

Feynman, Richard (1985). *QED: The Strange Theory of Light and Matter*. Princeton, New Jersey: Princeton University Press. ISBN: 0-691-08388-6.

Wikimedia Commons (June 2006). *Standard Model of Elementary Particles*. [Online; accessed February 6, 2018]. URL: https://upload.wikimedia.org/wikipedia/commons/0/00/Standard_Model_of_Elementary_Particles.svg.

Greensite, Jeff (2011). *Lecture Notes in Physics: An Introduction to the Confinement Problem*. 1st ed. Vol. 821. Springer-Verlag Berlin Heidelberg. ISBN: 978-3-642-14382-3. DOI: 10.1007/978-3-642-14382-3.

Wikimedia Commons (Apr. 2011). *QCD Phase Diagram*. [Online; accessed February 8, 2018]. URL: https://upload.wikimedia.org/wikipedia/commons/8/8f/QCD_phase_diagram.png.

Gross, David J. and Frank Wilczek (June 1973). "Ultraviolet Behavior of Non-Abelian Gauge Theories". In: *Phys. Rev. Lett.* 30 (26), pp. 1343–1346. DOI: 10.1103/PhysRevLett.30.1343. URL: https://link.aps.org/doi/10.1103/PhysRevLett.30.1343.

Politzer, H. David (June 1973). "Reliable Perturbative Results for Strong Interactions?" In: *Phys. Rev. Lett.* 30 (26), pp. 1346–1349. DOI: 10.1103/PhysRevLett.30.1346. URL: https://link.aps.org/doi/10.1103/PhysRevLett.30.1346.

Barger, Vernon D. and Roger J.N. Phillips (1997). *Collider Physics*. Reading, Massachusetts: Addison-Wesley Publishing Company. ISBN: 0-201-14945-1.

Bohr, Henrik and H.B. Nielsen (1977). "Hadron production from a boiling quark soup: A thermodynamical quark model predicting particle ratios in hadronic collisions". In: *Nuclear Physics B* 128.2, pp. 275–293. ISSN: 0550-3213. DOI: https://doi.org/10.1016/0550-3213(77)90032-3. URL: http://www.sciencedirect.com/science/article/pii/0550321377900323.

Alford, Mark G. et al. (Nov. 2008). "Color superconductivity in dense quark matter". In: *Rev. Mod. Phys.* 80 (4), pp. 1455–1515. DOI: 10.1103/RevModPhys.80.1455. URL: https://link.aps.org/doi/10.1103/RevModPhys.80.1455.

Allday, Jonathan (2002). *Quarks, Leptons and the Big Bang*. 2nd ed. Bristol, Philadelphia: Institute of Physics Pub. ISBN: 978-0-7503-0806-9.

The Nobel Prize in Physics 2013 (2014). URL: https://www.nobelprize.org/nobel_prizes/physics/laureates/2013/.

Carpenter, L. M. et al. (Mar. 2017). "Higgs boson decay to light jets at the LHC". In: 95.5, 053003, p. 053003. DOI: 10.1103/PhysRevD.95.053003. arXiv: 1611.05463 [hep-ph].

Adare, A. et al. (Jan. 2015). "An Upgrade Proposal from the PHENIX Collaboration". In: *ArXiv e-prints*. arXiv: 1501.06197 [nucl-ex].

sPHENIX collaboration (June 2017). "sPHENIX Forward Proposal – A Letter Of Intent". In: URL: https://www.sphenix.bnl.gov/web/system/files/sPH-cQCD-2017-001_draft_2017_06_02.pdf.

sPHENIX Collaboration (2018). *Intro | sPHENIX Collaboration*. URL: https://www.sphenix.bnl.gov/web/.

Particle Data Group, C. Patrignani et al. (2016).

Liboff, Richard L. (2011). *Kinetic theory: classical, quantum and relativistic descriptions*. Springer. Chap. 3.

Pinkenburg, Christopher H. (Sept. 2015). *Fun4All*. URL: https://www.jlab.org/conferences/eicsw/EICSoftwareMeeting-Pinkenberg-Fun4All.pdf.

CERN (n.d.). *ROOT a Data analysis Framework*. URL: https://root.cern.ch/.

RACF (Apr. 2014). *Condor at the RACF*. URL: https://www.racf.bnl.gov/docs/sw/condor/info.

Bazilevsky, Alexander (Nov. 2017). *sPHENIX Barrel EMCal: Clustering, Shower Profile, $\pi^0/\gamma/e$ Identification, as from sPHENIX G4 simulation*.